Blockade of KCa3.1 Ameliorates Renal Fibrosis Through the TGF-β1/Smad Pathway in Diabetic Mice

Chunling Huang,[1,2] Sylvie Shen,[1] Qing Ma,[1] Jason Chen,[3] Anthony Gill,[3] Carol A. Pollock,[1] and Xin-Ming Chen[1]

The Ca^{2+}-activated K^+ channel KCa3.1 mediates cellular signaling processes associated with dysfunction of vasculature. However, the role of KCa3.1 in diabetic nephropathy is unknown. We sought to assess whether KCa3.1 mediates the development of renal fibrosis in two animal models of diabetic nephropathy. Wild-type and $KCa3.1^{-/-}$ mice, and secondly $eNOS^{-/-}$ mice, had diabetes induced with streptozotocin and then were treated with/without a selective inhibitor of KCa3.1 (TRAM34). Our results show that the albumin-to-creatinine ratio significantly decreased in diabetic $KCa3.1^{-/-}$ mice compared with diabetic wild-type mice and in diabetic $eNOS^{-/-}$ mice treated with TRAM34 compared with diabetic mice. The expression of monocyte chemoattractant protein-1 (MCP-1), intercellular adhesion molecule 1 (ICAM1), F4/80, plasminogen activator inhibitor type 1 (PAI-1), and type III and IV collagen significantly decreased ($P < 0.01$) in kidneys of diabetic $KCa3.1^{-/-}$ mice compared with diabetic wild-type mice. Similarly, TRAM34 reduced the expression of the inflammatory and fibrotic markers described above in diabetic $eNOS^{-/-}$ mice. Furthermore, blocking the KCa3.1 channel in both animal models led to a reduction of transforming growth factor-β1 (TGF-β1) and TGF-β1 type II receptor (TβRII) and phosphorylation of Smad2/3. Our results provide evidence that KCa3.1 mediates renal fibrosis in diabetic nephropathy through the TGF-β1/Smad signaling pathway. Blockade of KCa3.1 may be a novel target for therapeutic intervention in patients with diabetic nephropathy. ***Diabetes* 62:2923–2934, 2013**

Diabetic nephropathy is a major cause of end-stage renal failure and premature mortality. Although strategies such as glycemic control, blood pressure control, and inhibition of the renin-angiotensin-aldosterone system have been shown to be effective to a limited extent, the number of patients with diabetes that ultimately develop progressive renal damage remains high (1,2). Therefore, it is of utmost importance to identify novel interventions for mitigating the progression of diabetic nephropathy.

Transforming growth factor-β1 (TGF-β1) has been identified as a key regulator of extracellular matrix (ECM) protein synthesis and degradation in diabetic nephropathy (3). TGF-β1 promotes renal fibrosis by upregulating genes encoding ECM proteins, leading to their increased synthesis, and at the same time enhances the production of inhibitors of ECM-degrading enzymes, such as plasminogen activator inhibitor type 1 (PAI-1) (4). TGF-β1 exerts its effects via binding to the membrane-bound TGF-β1 type II receptor (TβRII), causing the formation of heteromeric complexes. TβRII then transphosphorylates the type I receptor and activates the Smad signaling pathway to modulate gene transcription by phosphorylating Smad2/3. In addition, the accumulation of inflammatory cells and upregulated expression of proinflammatory mediators such as monocyte chemoattractant protein-1 (MCP-1) and intercellular adhesion molecule 1 (ICAM1) contribute to the development of renal fibrosis in human and animal models of diabetic nephropathy (5).

Accumulated evidence indicates that calcium signaling cascades play a critical role in the functional activity of diverse tissues. Modification of the activity of Ca^{2+}-activated K^+ channels (KCa) leads to changes in the cellular and ultrastructural membrane potentials required for various cellular processes (6). KCa3.1 (also known as IK1, SK4, or KCNN4) belongs to the potassium intermediate/small conductance calcium-activated channel family. The intermediate-conductance KCa3.1 channel was first described by Gardos in erythrocytes in 1958 (7) and was subsequently cloned from pancreas, placenta, and lymphoid tissue in 1997 (8–10). KCa3.1 proteins are distributed in the membranes of both cytoplasm and mitochondria. KCa3.1 regulates K^+ efflux, increasing the driving force for Ca^{2+} entry through hyperpolarization of the plasma membrane (11). KCa3.1-mediated Ca^{2+} influx is associated with inflammation, atherogenesis, and proliferation of endothelial cells, T lymphocytes, macrophages, and fibroblasts (12–16). KCa3.1 is a potential molecular target for pharmacological intervention in vascular restenosis, urinary incontinence, prostate cancer, and autoimmune disease (17–19). Recently, Grgic et al. have reported that the highly selective inhibitor of KCa3.1, TRAM34 (20,21), can reduce renal fibrosis in animal models of obstructive uropathy (22) and prevent acute kidney transplant rejection in rats if given in combination with a Kv1.3 blocker (23). However, the role of KCa3.1 in diabetic nephropathy has not been studied.

In this study, we investigated the therapeutic potential of KCa3.1 in diabetic nephropathy using two mouse models of streptozotocin (STZ)-induced diabetes. Our results demonstrate that blockade of KCa3.1 was able to ameliorate albuminuria and minimize renal damage induced by diabetes. Furthermore, our results describe an additional mechanism for KCa3.1-mediated protection through the negative regulation of the TGF-β1 and Smad pathway.

RESEARCH DESIGN AND METHODS

Materials. Recombinant human TGF-β1 and the selective KCa3.1 blocker TRAM34 {1-[(2-chlorophenyl) diphenylmethyl]-^{1}H-pyrazole} were purchased from R&D Systems (Minneapolis, MN) and Sigma-Aldrich (St. Louis, MO),

From the [1]Kolling Institute of Medical Research, Royal North Shore Hospital, Sydney Medical School, and University of Sydney, St Leonards, Sydney, New South Wales, Australia; the [2]Xiamen Center of Clinical Laboratory, Xiamen Zhongshan Hospital, Medical College of Xiamen University, Xiamen, China; and the [3]Department of Anatomical Pathology, Royal North Shore Hospital, St Leonards, Sydney, New South Wales, Australia.
Corresponding author: Carol A. Pollock, carol.pollock@sydney.edu.au.
Received 25 January 2013 and accepted 26 March 2013.
DOI: 10.2337/db13-0135

See accompanying commentary, p. 2648.

TABLE 1
Nucleotide sequence of the primers used for qRT-PCR

Species	Molecules	Forward primer (5′-3′)	Reverse primer (5′-3′)
Human	COL3	CTGGACCCCAGGGTCTTC	GACCATCTGATCCAGGGTTTC
	COL4	CGGGTACCCAGGACTCATAG	GGACCTGCTTCACCCTTTTC
	GAPDH	AGCCACATCGCTCAGACAC	GCCCAATACGACCAAATCC
	PAI-1	TCCAGCAGCTGAATTCCTG	GCTGGAGACATCTGCATCCT
	TβRII	TCCATCTGTGAGAAGCCACA	GGGTCATGGCAAACTGTCTC
Mice	β-actin	CAGCTGAGAGGGAAATCGTG	CGTTGCCAATAGTGATGACC
	COL3	TCCCCTGGAATCTGTGAATC	TGAGTCGAATTGGGGAGAAT
	COL4	TTAAAGGACTCCAGGGACCAC	CCCACTGAGCCTGTCACAC
	F4/80	CCTGGACGAATCCTGTGAAG	GGTGGGACCACAGAGAGTTG
	ICAM1	GCTACCATCACCGTGTATTCG	TGAGGTCCTTGCCTACTTGC
	MCP-1	GCCTGCTGTTCACAGTTGC	CAGGTGAGTGGGGCGTTA
	PAI-1	AGGATCGAGGTAAACGAGAGC	GCGGGCTGAGATGACAAA
	TGF-β1	TCAGACATTCGGGAAGCAGT	ACGCCAGGAATTGTTGCTAT
	TβRII	GGCTCTGGTACTCTGGGAAA	AATGGGGGCTCGTAATCCT

respectively. Anti-KCa3.1 was purchased from Abnova (Taipei City, Taiwan). Anti–PAI-1, –TGF-β1, and –TβRII were purchased from BD Biosciences (Franklin Lakes, NJ), LifeSPAN (Seattle, WA), and Upstate (Billerica, MA). Anti–type III collagen (COL3) and –type IV collagen (COL4) were obtained from Abcam (Cambridge, MA). Anti–α-tubulin antibody was from Sigma-Aldrich. Anti–phospho-Smad2, –phospho-Smad3, and -Smad2/3 were purchased from Cell Signaling Technology (Danvers, MA). Anti-F4/80 was obtained from AbD Serotec (Oxford, U.K.).

Human kidney biopsies. Human kidney biopsy specimens from patients with diabetic nephropathy were provided by the Department of Anatomical Pathology of the Royal North Shore Hospital. Kidneys removed from patients, generally due to peripheral tumor but without known kidney disease, served as controls. This study was approved by the Human Research Ethics Committee of the Royal North Shore Hospital.

Animal studies. KCa3.1$^{-/-}$ mice were provided by Dr. James Melvin (National Institute of Dental and Craniofacial Research, Bethesda, MD). Eight-week-old male KCa3.1$^{+/+}$ (C57B/6), KCa3.1$^{-/-}$, and eNOS$^{-/-}$ mice (The Jackson Laboratory, Bar Harbor, ME) weighing ~20–25 g were assigned to receive either 55 mg/kg STZ (Sigma-Aldrich) diluted in 0.1 mol/L citrate buffer, pH 4.5, or citrate buffer alone by intraperitoneal injection as described previously (24). A group of KCa3.1$^{+/+}$ (n = 8) and eNOS$^{-/-}$ mice (n = 6) that received citrate buffer alone served as nondiabetic controls. eNOS$^{-/-}$ diabetic mice were then randomized into two groups: those receiving treatment with TRAM34, 120 mg/kg/day intraperitoneally, and those receiving vehicle (DMSO) alone for 24 weeks. Treatment commenced within 24 h of the last STZ injection. All animals were housed in the Kearns Animal Facility of the Kolling Institute of Medical Research, with a stable environment maintained at 22 ± 1°C with a 12/12-h light-dark cycle.

Mice were weighed and their blood glucose levels were measured using the ACCU-CHEK glucometer (Roche Diagnostics) weekly, and only STZ-treated animals with blood glucose >16 mmol/L were considered diabetic. Systolic blood pressure was noninvasively measured using a volume pressure recording sensor and an occlusion tail cuff (CODA System). Diabetic mice received insulin (Lantus, Frankfurt, Germany) treatment to prevent ketosis. At the time they were killed, spot urine and 24-h urine were collected and then the weight of kidney and body was recorded. Urine albumin and creatinine levels were determined with Murine Microalbuminuria ELISA kit and Creatinine Companion kit (Exocell Inc., Philadelphia, PA). After animals were culled, left kidneys were removed and snap frozen for the isolation of RNA or protein, and right kidneys were perfused with PBS and fixed in 10% buffered formalin for histological examination. Experimental procedures adhered to the guidelines of the National Health and Medical Research Council of Australia's Code for the Care and Use of Animals for Scientific Purposes and were approved by the Animal Research Ethics Committee of the Royal North Shore Hospital.

Cell culture. Human proximal tubular cells (HK2 cells) were grown in keratinocyte serum-free medium (Invitrogen, Carlsbad, CA). The cells were exposed to TGF-β1 (2 ng/mL) in the presence or absence of TRAM34 (4 μmol/L) (21) for 48 h, and then the culture supernatant and cell lysates were collected, respectively. In all experiments, cells were serum starved overnight before adding TGF-β1 and TRAM34.

KCa3.1 silencing. HK2 cells were transfected with either siRNA targeting KCa3.1 or negative control siRNA using Lipofectamine 2000 reagent (Invitrogen) according to the manufacturer's instructions. The targeting siRNA sequence for KCa3.1 is 5′-GCACCUUUCAGACACACUU-3′ (GenePharma, Shanghai, China). After transfection, the cells were treated with TGF-β1 for 48 h. Cell culture supernatant and cell lysates were then collected for further analysis.

RNA isolation and RT-PCR analysis. Total RNA was extracted from cells and mouse kidneys using GenElute Mammalian Total RNA Miniprep Kit (Sigma-Aldrich) or Trizol (Invitrogen), respectively. The cDNA was synthesized using SuperScript VILO cDNA Synthesis Kit (Invitrogen). Quantitative real-time PCR was performed using the SYBR Green PCR Master Mix kit (Invitrogen) with the intron-spanning primers as shown in Table 1 on the ABI-Prism-7900 Sequence Detection System (Applied Biosystems). The relative mRNA expression levels were calculated according to the $2^{-\Delta\Delta Ct}$ method (25). The mRNA expression of β-actin was used as the endogenous reference control.

Western blot analysis. Type III and IV collagen were measured in cell culture supernatant, and cell lysates were prepared in RIPA buffer with protease inhibitors (Roche, Mannheim, Germany).

Samples were separated by SDS-PAGE and then transferred to Hybond ECL nitrocellulose membrane (Amersham, Piscataway, NJ). The membranes were incubated with primary antibodies PAI-1 (1:1,000), collagen III (1:1,000), collagen IV (1:5,000), phospho-Smad2 (1:1,000), phospho-Smad3 (1:1,000), and Smad2/3 (1:1,000) at 4°C overnight followed by horseradish peroxidase–conjugated secondary antibody (1:5,000; Amersham). The blots were then detected with standard enhanced chemiluminescence technique, and the bands were quantified by densitometry using the LAS-4000 Imaging System (Fujifilm, Tokyo, Japan).

Histology and immunohistochemistry. Paraffin-embedded and frozen kidney sections were used for immunohistochemical staining. Matrix deposition within the interstitium was assessed using Masson's trichrome stain (American

TABLE 2
Metabolic and physiological parameters of KCa3.1$^{+/+}$ and KCa3.1$^{-/-}$ mice

	KCa3.1$^{+/+}$ control	KCa3.1$^{+/+}$ DM	KCa3.1$^{-/-}$ DM
Blood glucose level (mmol/L)	8.554 ± 0.223	22.69 ± 0.647‡	23.17 ± 0.665‡
Body weight (g)	30.3 ± 0.693	23.97 ± 0.983‡	29.81 ± 0.549§
Kidney/body weight (mg/g)	6.435 ± 0.194	9.344 ± 0.423‡	8.16 ± 0.279§
Blood pressure (systolic, mmHg)	110.9 ± 2.424	109.5 ± 1.609	107.2 ± 1.890
Spot albumin-to-creatinine ratio (mg/mg)	1.293 ± 0.345	4.947 ± 0.970‡	2.29 ± 0.634§
Albumin-to-creatinine ratio (mg/mg/24 h)	1.096 ± 0.253	4.169 ± 0.252‡	2.298 ± 0.695§

Data are presented as mean ± SEM. DM, diabetes mellitus. ‡$P < 0.05$, vs. KCa3.1$^{+/+}$ control. §$P < 0.05$, vs. KCa3.1$^{+/+}$ DM.

TABLE 3
Metabolic and physiological parameters of eNOS$^{-/-}$ control and diabetic mice treated with TRAM34 or vehicle

	Control	DM+DMSO	DM+TRAM34
Blood glucose level (mmol/L)	11.45 ± 0.202	27.33 ± 1.248*	28.46 ± 1.305*
Body weight (g)	26.58 ± 0.396	21.9 ± 0.300*	21.46 ± 0.473*
Kidney/body weight (mg/g)	6.026 ± 0.298	8.76 ± 0.439*	7.432 ± 0.351†
Blood pressure (systolic, mmHg)	193.4 ± 3.779	190.9 ± 8.839	186 ± 1.155
Spot albumin-to-creatinine ratio (mg/mg)	0.904 ± 0.072	2.547 ± 0.532*	1.22 ± 0.113†
Albumin-to-creatinine ratio (mg/mg/24 h)	0.897 ± 0.116	2.225 ± 0.433*	1.326 ± 0.247†

Data are presented as mean ± SEM. DM, diabetes mellitus. *$P < 0.05$, vs. control. †$P < 0.05$, vs. DM+DMSO.

MasterTech, Lodi, CA). In brief, endogenous peroxidase activity was blocked by incubation in 0.3% hydrogen peroxide. After preincubation with 10% protein block (Dako, Carpinteria, CA) for 10 min at room temperature to block nonspecific binding of antibodies, the tissues were incubated overnight at 4°C with primary antibodies against KCa3.1, F4/80, type III and IV collagen, TGF-β1, TβRII, and phospho-Smad2/3. After incubation with the appropriate secondary antibodies, sections were developed with 3,3-diaminobenzidine (Dako) to produce a brown color and counterstained with hematoxylin. Positive signals in the renal cortex regions were quantified using Image J software as previously described (26). The number of cells positive for F4/80$^+$ and phospho-Smad2/3$^+$ was counted in 10 high-power fields (HPFs) (40×) of the tubulointerstitium.

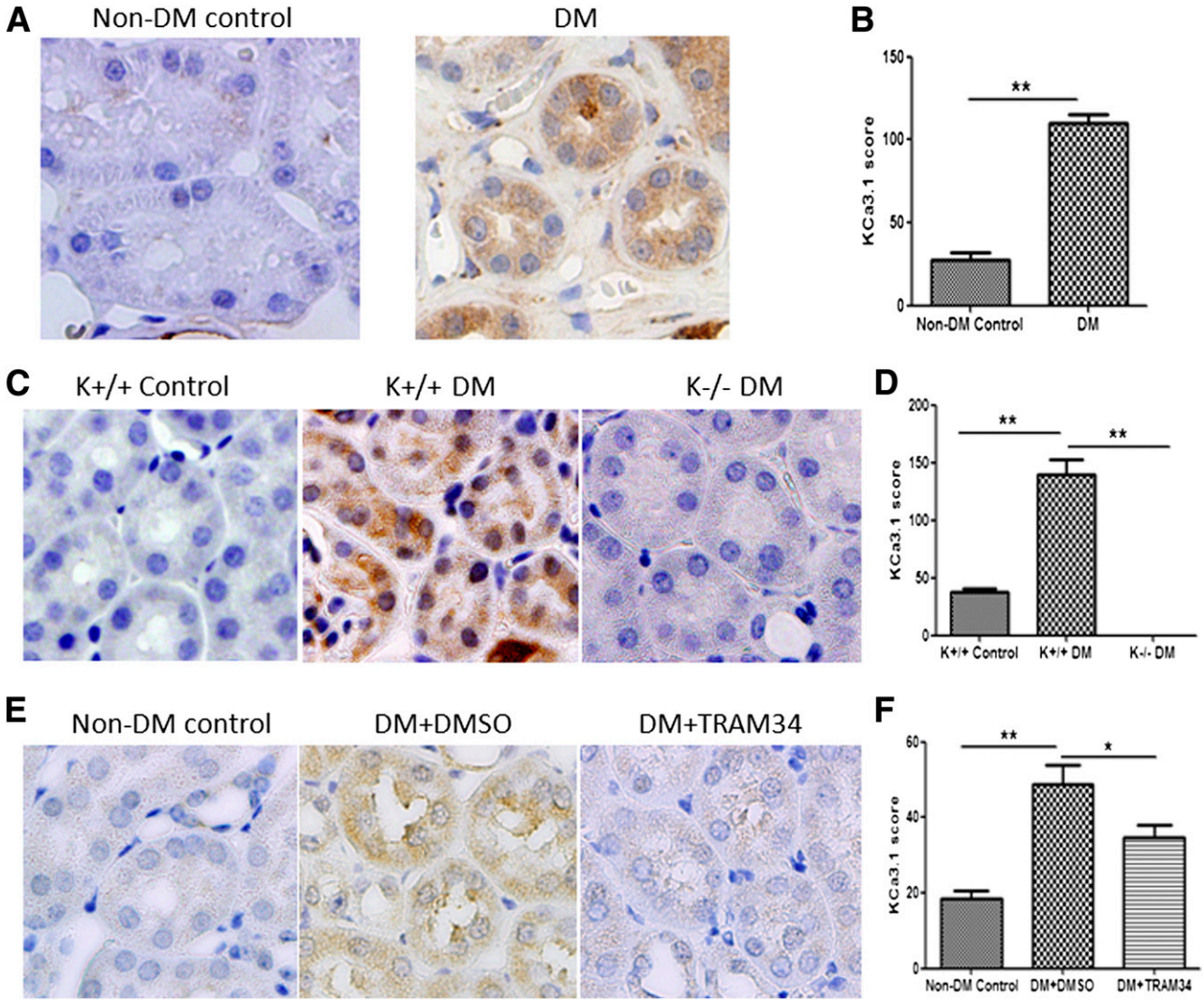

FIG. 1. KCa3.1 expression was increased in kidneys of human and mice with diabetic nephropathy. *A*: Immunohistochemical analysis demonstrated increased KCa3.1 expression in kidney biopsies from patients with diabetic nephropathy (diabetes mellitus [DM]) compared with nondiabetic control kidneys (non-DM control) (n = 8). *B*: The quantitation of KCa3.1 expression in human biopsies. *C*: Immunohistochemical analysis demonstrated that the expression of KCa3.1 was increased in kidneys of diabetic KCa3.1$^{+/+}$ mice compared with normal mice. There is no KCa3.1 expression in KCa3.1$^{-/-}$ mice (n = 8). *E*: Immunohistochemical analysis demonstrated increased KCa3.1 expression in kidneys of diabetic eNOS$^{-/-}$mice (DM+DMSO) compared with normal mice (non-DM control), and TRAM34 suppressed KCa3.1 expression in the kidneys of diabetic eNOS$^{-/-}$mice (DM +TRAM34) (n = 6). *D* and *F*: The quantitation of KCa3.1 expression in mouse kidney. Results are presented as mean ± SEM. *$P < 0.05$; **$P < 0.01$. Original magnification ×400.

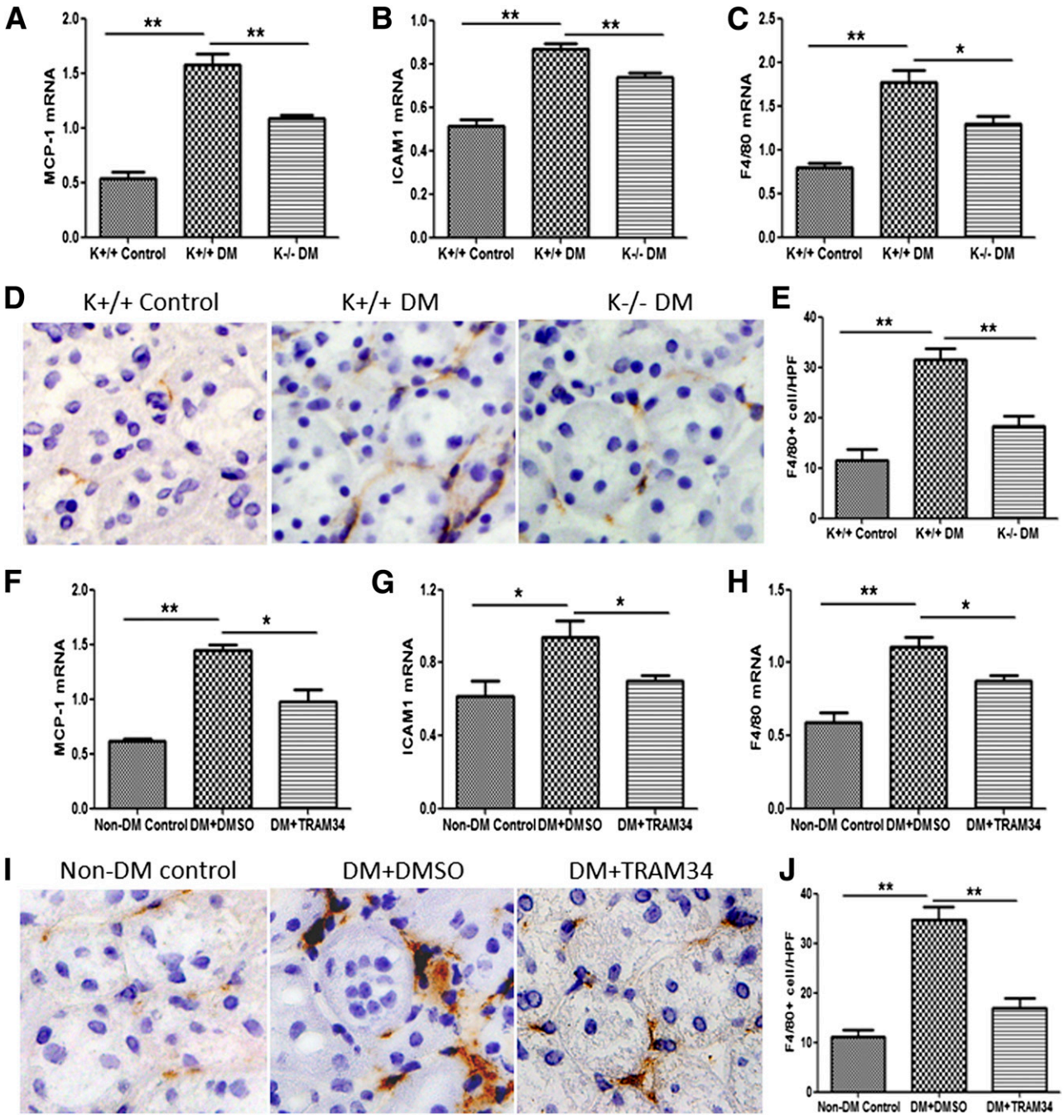

FIG. 2. Blockade of KCa3.1 reversed MCP-1, ICAM1, and F4/80 expression in diabetic kidneys. Quantitative RT-PCR showed increased mRNA levels of MCP-1 (*A*), ICAM1 (*B*), and F4/80 (*C*) in the kidneys of diabetic KCa3.1$^{+/+}$ mice but the reverse in diabetic KCa3.1$^{-/-}$ mice (n = 8). *D*: Immunohistochemical analysis showed increased F4/80 in diabetic KCa3.1$^{+/+}$ kidneys compared with control mice and reversed expression of F4/80 in diabetic KCa3.1$^{-/-}$ kidneys (n = 8). Quantitative RT-PCR showed increased mRNA levels of MCP-1 (*F*), ICAM1 (*G*), and F4/80 (*H*) in the kidneys of diabetic eNOS$^{-/-}$ mice but the reverse in diabetic mice treated with TRAM34 (n = 6). *I*: Immunohistochemical analysis showed increased F4/80 in diabetic eNOS$^{-/-}$ kidneys compared with control mice and reversed expression of F4/80 in diabetic kidneys treated with TRAM34 (n = 6). *E* and *J*: The quantitation of F4/80 expression in mouse kidney. Results are presented as mean ± SEM. *P < 0.05; **P < 0.01. Original magnification ×400. DM, diabetes mellitus.

Statistical analysis. The results from at least four independent experiments were expressed as mean ± SEM. Statistical analysis of data from two groups was compared by two-tailed Student t test. Data from multiple groups were analyzed by one-way ANOVA, followed by Tukey post hoc test. Statistical significance was determined as $P < 0.05$.

RESULTS

Blockade of KCa3.1 attenuates the renal injury in two models of STZ-induced diabetes. To examine the role of KCa3.1 in the development of diabetic nephropathy in vivo, we conducted two animal studies: wild-type KCa3.1$^{+/+}$ and KCa3.1$^{-/-}$ mice and secondly eNOS$^{-/-}$ mice with or without administration of TRAM34. The diabetic eNOS$^{-/-}$ mice are endorsed by the Animal Models of Diabetic Complications Consortium (AMDCC) for studies in diabetic nephropathy (27). As shown in Table 2, diabetic wild-type (KCa3.1$^{+/+}$) mice showed significantly increased blood glucose levels and reduced body weight compared

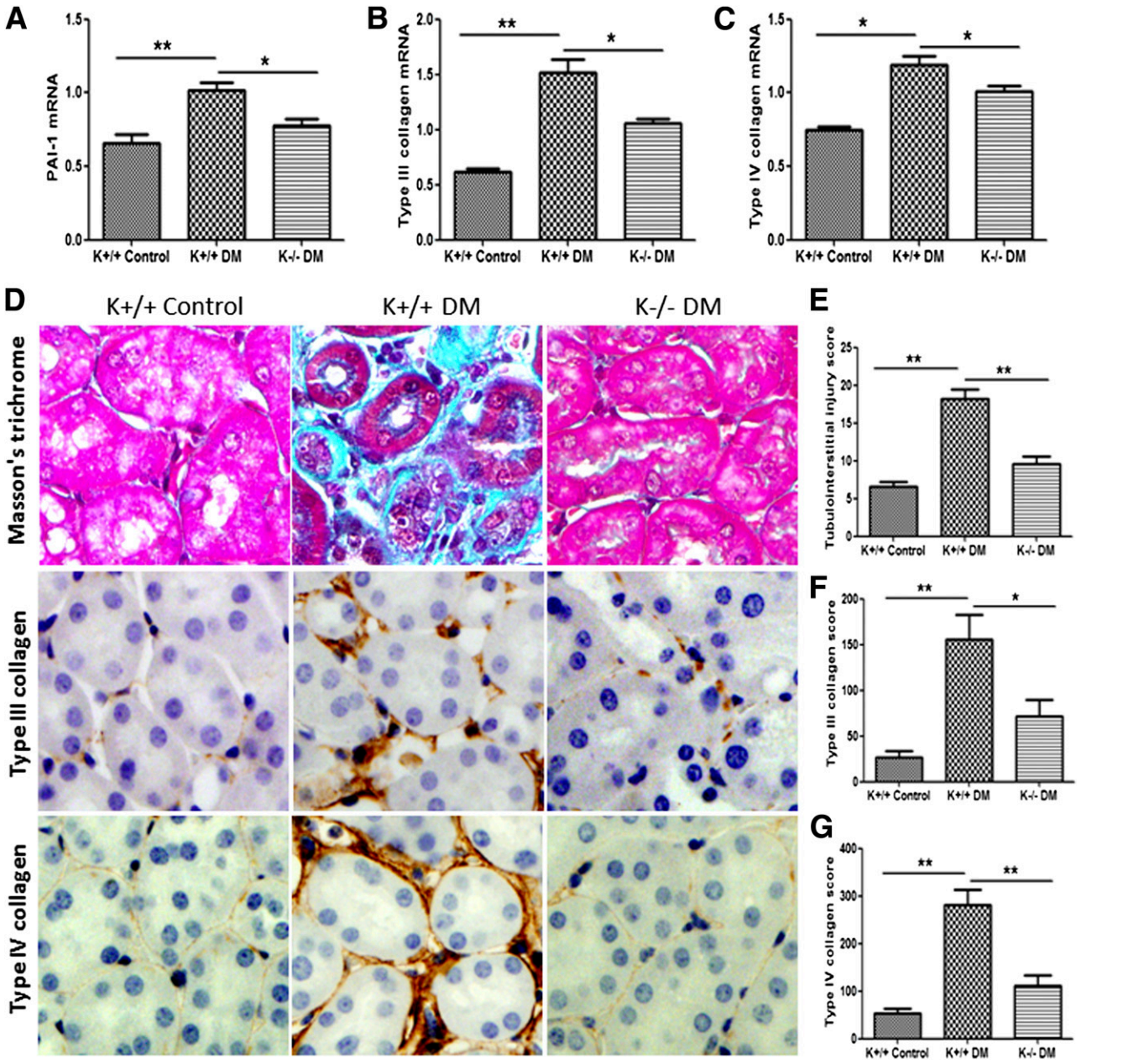

FIG. 3. Blockade of KCa3.1 suppressed the overexpression of ECM in diabetic kidneys. Quantitative RT-PCR showed increased mRNA expression of PAI-1 (*A*) and type III (*B*) and IV collagen (*C*) in the kidneys of diabetic KCa3.1$^{+/+}$ mice compared with control mice but reduced mRNA expression in diabetic KCa3.1$^{-/-}$ kidneys (n = 8). Representative images (*D*) show Masson's trichrome and immunohistochemical staining of type III and IV collagen in the renal cortex from control KCa3.1$^{+/+}$, diabetic KCa3.1$^{+/+}$, and diabetic KCa3.1$^{-/-}$ mice (n = 8). Quantitative RT-PCR showed increased mRNA expression of PAI-1 (*H*) and type III (*I*) and IV collagen (*J*) in the kidneys of diabetic eNOS$^{-/-}$ mice compared with control mice but reduced mRNA expression with TRAM34 treatment (DM+TRAM34) (n = 6). Representative images (*K*) show Masson's trichrome and immunohistochemical staining of type III and IV collagen in the renal cortex from control, diabetic, and diabetic mice treated with TRAM34. The degree of tubulointerstitial injury (*E* and *L*) and the quantitation of type III (*F* and *M*) and IV collagen (*G* and *N*) were determined by computer-based morphometric analysis. Results are presented as mean ± SEM. *P < 0.05; **P < 0.01. Original magnification ×400. DM, diabetes mellitus.

with the control group. The mean kidney–to–body weight ratio in diabetic KCa3.1$^{+/+}$ mice was significantly higher than that of control ($P < 0.05$), which was reduced in diabetic KCa3.1 $^{-/-}$ mice ($P < 0.05$). There was no difference in the blood pressure observed between control and diabetic mice. To determine renal function, spot urine albumin-to-creatinine ratio and 24-h urine albumin-to-creatinine ratio were measured at the time the mice were killed. Renal function was impaired in diabetic KCa3.1$^{+/+}$ mice, and this impairment was significantly attenuated in KCa3.1$^{-/-}$ mice ($P < 0.05$). Similar results were found with pharmacological inhibition of KCa3.1 in diabetic eNOS$^{-/-}$ mice by administrating the specific inhibitor TRAM34 (Table 3). TRAM34 did not affect glucose levels or weight gain. Treatment of diabetic animals with TRAM34 significantly alleviated all indices of renal injury in eNOS$^{-/-}$ mice. These results indicate that blockade of KCa3.1 attenuates renal injury caused by diabetes, implicating the essential role of KCa3.1 in STZ-induced diabetic nephropathy.

KCa3.1 expression is increased in kidney tissues of humans and mice with diabetic nephropathy. To investigate whether KCa3.1 expression is altered in diabetic

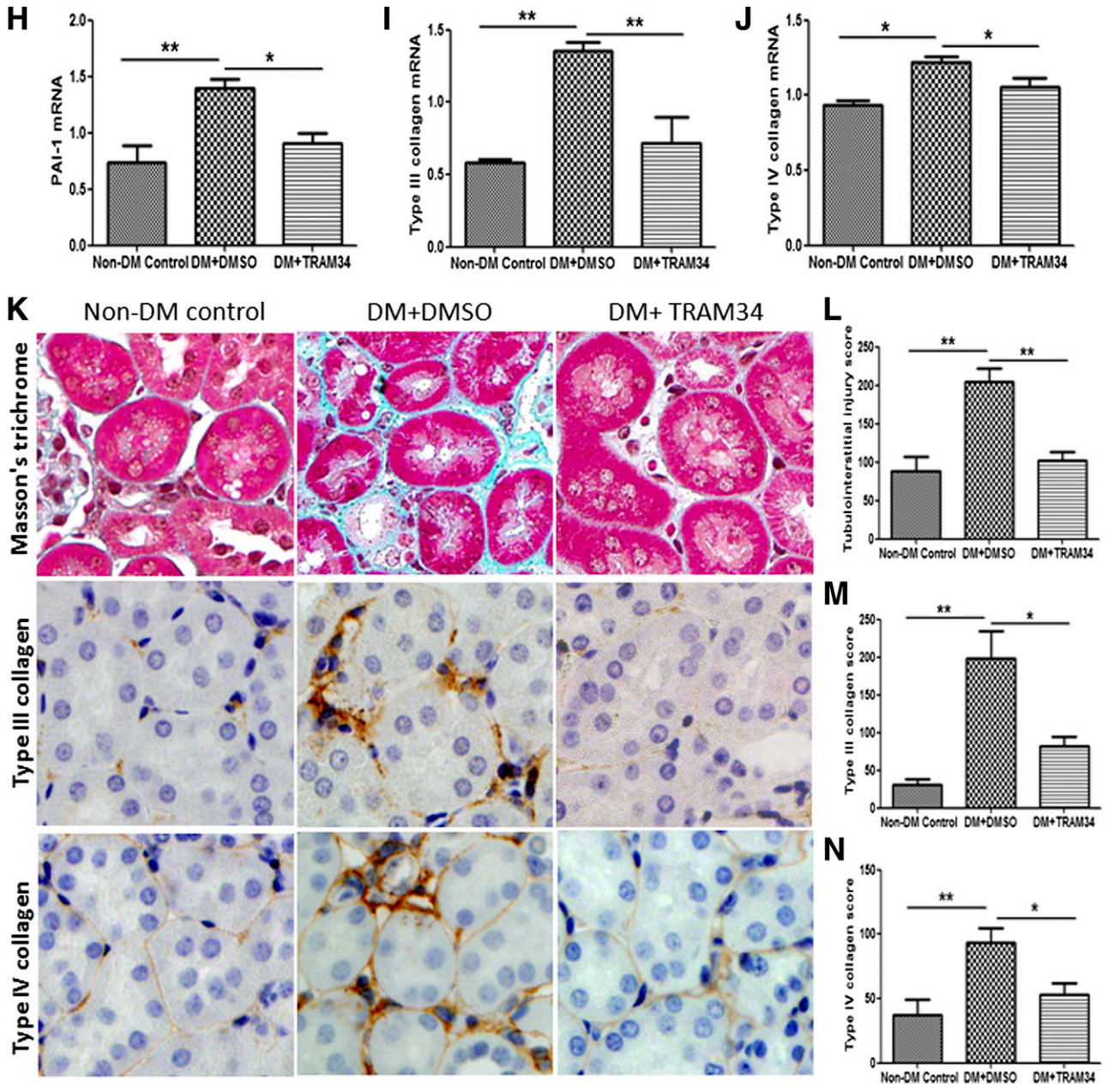

FIG. 3. Continued.

nephropathy, we first examined the expression of KCa3.1 in kidney biopsies from patients with diabetic nephropathy and nondiabetic controls using immunohistochemical analysis. As shown in Fig. 1*A*, considerable staining for the KCa3.1 channel protein was observed in kidney proximal tubular cells of diabetic kidneys, whereas only a low basal level of KCa3.1 was expressed in nondiabetic controls ($P < 0.01$) (Fig. 1*B*).

We next determined the expression of KCa3.1 in two STZ diabetic mice models as described above. As shown in Fig. 1*C* and *D*, a low basal level of KCa3.1 expression was observed in kidney proximal tubular cells of nondiabetic KCa3.1$^{+/+}$ mice, which was significantly upregulated in most proximal tubular cells of diabetic KCa3.1$^{+/+}$ mice ($P < 0.01$). As expected, there was no KCa3.1 expression in KCa3.1-deficient diabetic mice. Similarly, the administration of TRAM34 significantly reversed the upregulated KCa3.1 expression in proximal tubular cells of diabetic eNOS$^{-/-}$ mice compared with that in the vehicle-treated group ($P < 0.01$) (Fig. 1*E* and *F*). Collectively, these data provided evidence for substantial KCa3.1 upregulation in diabetic kidneys, indicating a potential pathophysiological involvement of the KCa3.1 channel in diabetic nephropathy.

Blockade of KCa3.1 prevents inflammatory responses in diabetic mice. To characterize the role of KCa3.1 in the regulation of inflammation, we examined two proinflammatory cytokines, MCP-1 and ICAM1, and one macrophage marker, F4/80, in kidney tissues. RT-PCR analyses of kidney tissues demonstrated that the expressions of MCP-1, ICAM1, and F4/80 were increased by 2.9-, 1.7-, and 2.2-fold, respectively, in the diabetic KCa3.1$^{+/+}$ group, which were reduced in the diabetic KCa3.1$^{-/-}$ group ($P < 0.05$) (Fig. 2*A–C*). Remarkably, histopathological analysis of renal cross-sections demonstrated a 52% reduction of F4/80

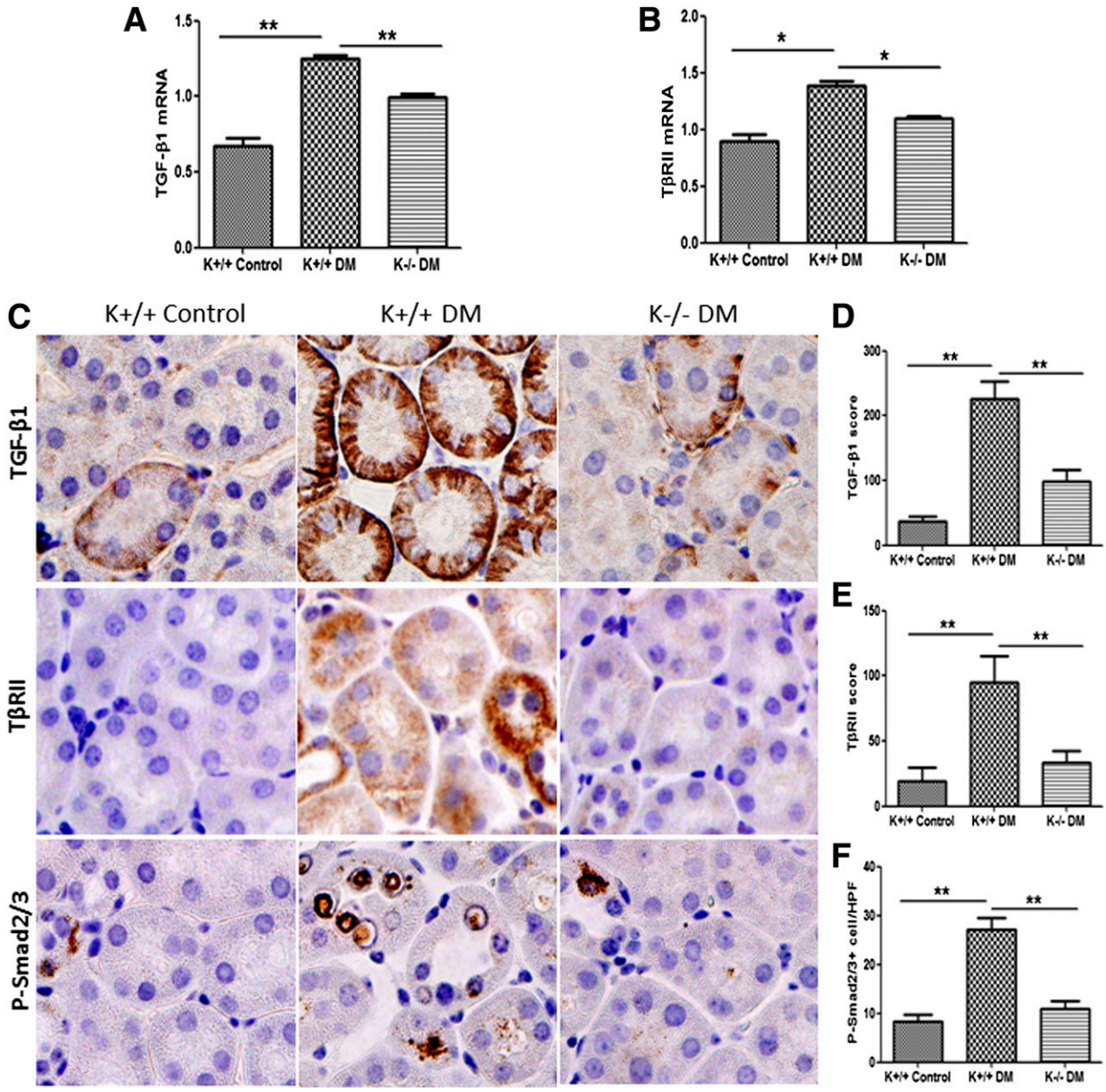

FIG. 4. Blockade of KCa3.1 reversed TGF-β1, TβRII, and phospho (P)-Smad2/3 expression in diabetic nephropathy. Quantitative RT-PCR showed increased mRNA expression of TGF-β1 (*A*) and TβRII (*B*) in the kidneys of diabetic KCa3.1$^{+/+}$ mice compared with control mice but reduced mRNA expression in diabetic KCa3.1$^{-/-}$ kidneys (n = 8). *C*: Immunohistochemical staining of TGF-β1, TβRII, and P-Smad2/3 in the renal cortex from control KCa3.1$^{+/+}$, diabetic KCa3.1$^{+/+}$, and diabetic Kca3.1$^{-/-}$ mice (n = 8). Quantitative RT-PCR showed increased mRNA expression of TGF-β1 (*G*) and TβRII (*H*) in the kidneys of diabetic eNOS$^{-/-}$ mice compared with control mice but reduced mRNA expression in diabetic kidneys treated with TRAM34 (n = 6). *I*: Immunohistochemical staining of TGF-β1, TβRII, and P-Smad2/3 in the renal cortex from control, diabetic, and diabetic mice treated with TRAM34 (n = 6). The quantitation of TGF-β1 (*D* and *J*), TβRII (*E* and *K*), and P-Smad2/3 (*F* and *L*) expression in mouse kidney. Results are presented as mean ± SEM. *P < 0.05; **P < 0.01. Original magnification ×400. DM, diabetes mellitus.

expression in diabetic kidneys of KCa3.1-deficient animals as compared with diabetic KCa3.1$^{+/+}$ controls ($P < 0.01$) (Fig. 2*D* and *E*). Consistent with this finding, we also observed a significant decrease in MCP-1, ICAM1, and F4/80 expression in the kidneys of diabetic eNOS$^{-/-}$ mice treated with the KCa3.1 blocker TRAM34 compared with the control group ($P < 0.05$) (Fig. 2*F*–*J*). These data suggest that KCa3.1 contributes to the production of proinflammatory cytokines and macrophage infiltration in diabetic nephropathy.

Blockade of KCa3.1 reduces PAI-1 expression and ECM deposition in diabetic mice. To determine whether KCa3.1 is involved in the regulation of renal fibrosis that is inherent in diabetes, we evaluated the effect of KCa3.1 on the expression of PAI-1 and type III and IV collagen. As indicated in Fig. 3*A*–*C*, a marked induction of PAI-1 (1.5-fold, $P < 0.01$) and type III (2.4-fold, $P < 0.01$) and IV (1.6-fold, $P < 0.05$) collagen mRNA was observed in the kidneys of diabetic KCa3.1$^{+/+}$ animals when compared with nondiabetic controls. KCa3.1 deficiency significantly inhibited the expression of PAI-1 and type III and IV collagen in diabetic kidneys. In addition, we also examined the effect of KCa3.1 on the expression of interstitial collagen fibrils by Masson's trichrome staining and type III and IV collagen by immunohistochemical staining. In KCa3.1$^{+/+}$ mice, an increase in collagen accumulation and deposition

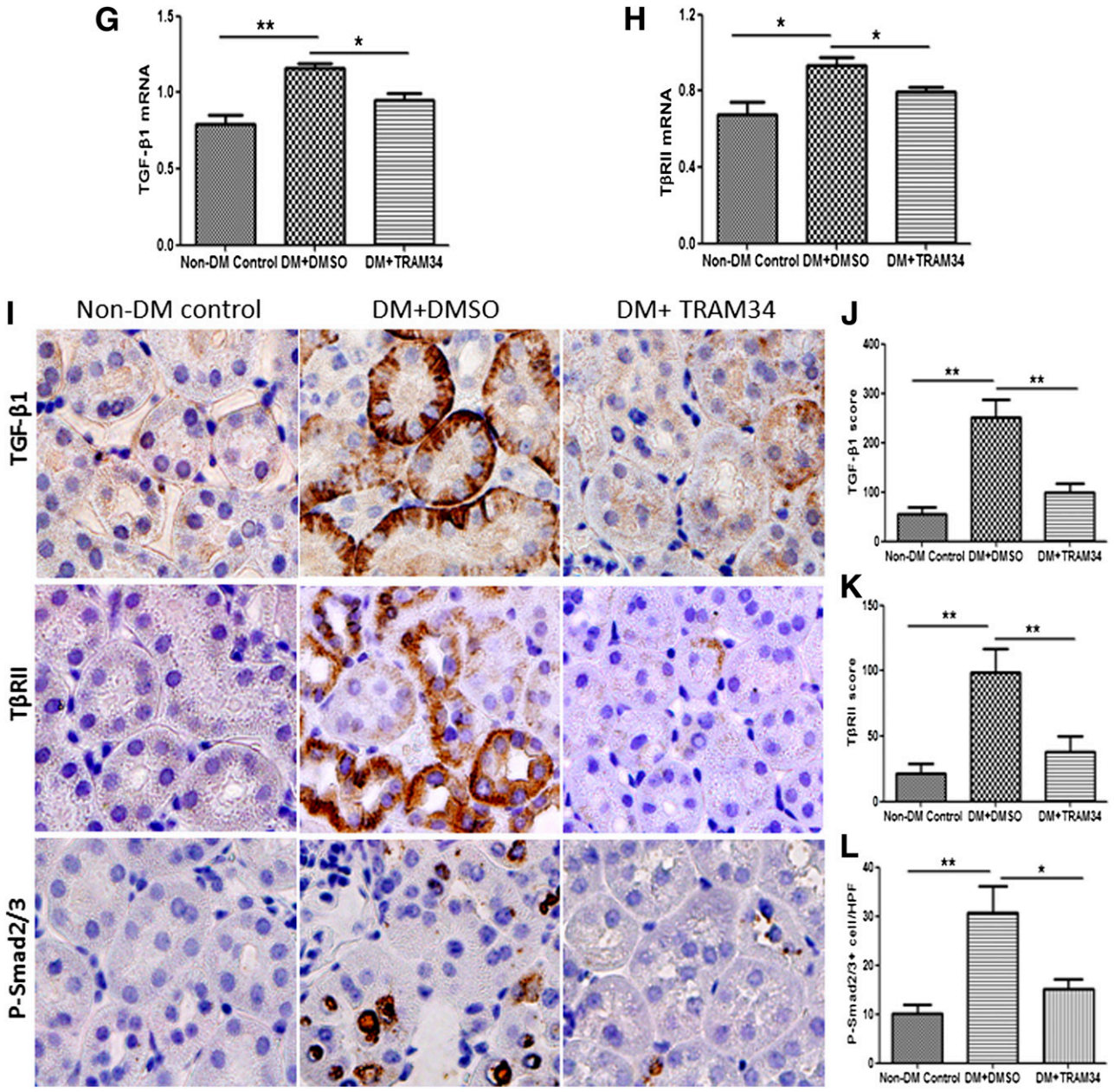

FIG. 4. Continued.

was observed within the tubulointerstitium after induction of diabetes. KCa3.1 deficiency significantly reduced excess matrix deposition ($P < 0.01$) (Fig. 3*D* and *E*). Diabetes also resulted in increased expression of type III ($P < 0.05$) (Fig. 3*D* and *F*) and IV collagen ($P < 0.01$) (Fig. 3*D* and *G*), whereas KCa3.1 deficiency attenuated this response. In line with these observations, renal gene expression levels of established fibrotic markers (PAI-1 and type III and IV collagen) were considerably lower in diabetic kidneys from TRAM34-treated mice compared with vehicle-treated mice ($P < 0.05$) (Fig. 3*H*–*J*). Consistently, the administration of TRAM34 significantly reversed tubulointerstitial damage in diabetic kidneys as compared with vehicle-treated controls ($P < 0.01$) (Fig. 3*K* and *L*). Furthermore, the immunohistochemical staining also showed a substantially increased abundance of immunostainable type III ($P < 0.05$) (Fig. 3*K* and *M*) and IV collagen ($P < 0.05$) (Fig. 3*K* and *N*) localized in the interstitial areas of diabetic kidneys compared with controls, which was reversed after TRAM34 treatment. Collectively, these results indicate that blockade of KCa3.1 suppresses interstitial matrix production and reduces renal interstitial fibrosis in diabetic nephropathy.

Blockade of KCa3.1 inhibits the expression of TGF-β1 and TβRII and phosphorylation of Smad2/3 in diabetic mice. Increased expression of TGF-β1 and/or TGF-β receptors is found in almost all forms of kidney diseases with interstitial fibrosis (28). To elucidate the mechanisms by which blockade of KCa3.1 inhibited renal fibrosis, we examined the effects of KCa3.1 on the expression of TGF-β1 and TβRII in diabetic kidneys using real-time PCR and immunohistochemical staining. At both mRNA and protein levels, expression of TGF-β1 and TβRII was significantly increased in diabetic KCa3.1$^{+/+}$ mice compared with control groups, and

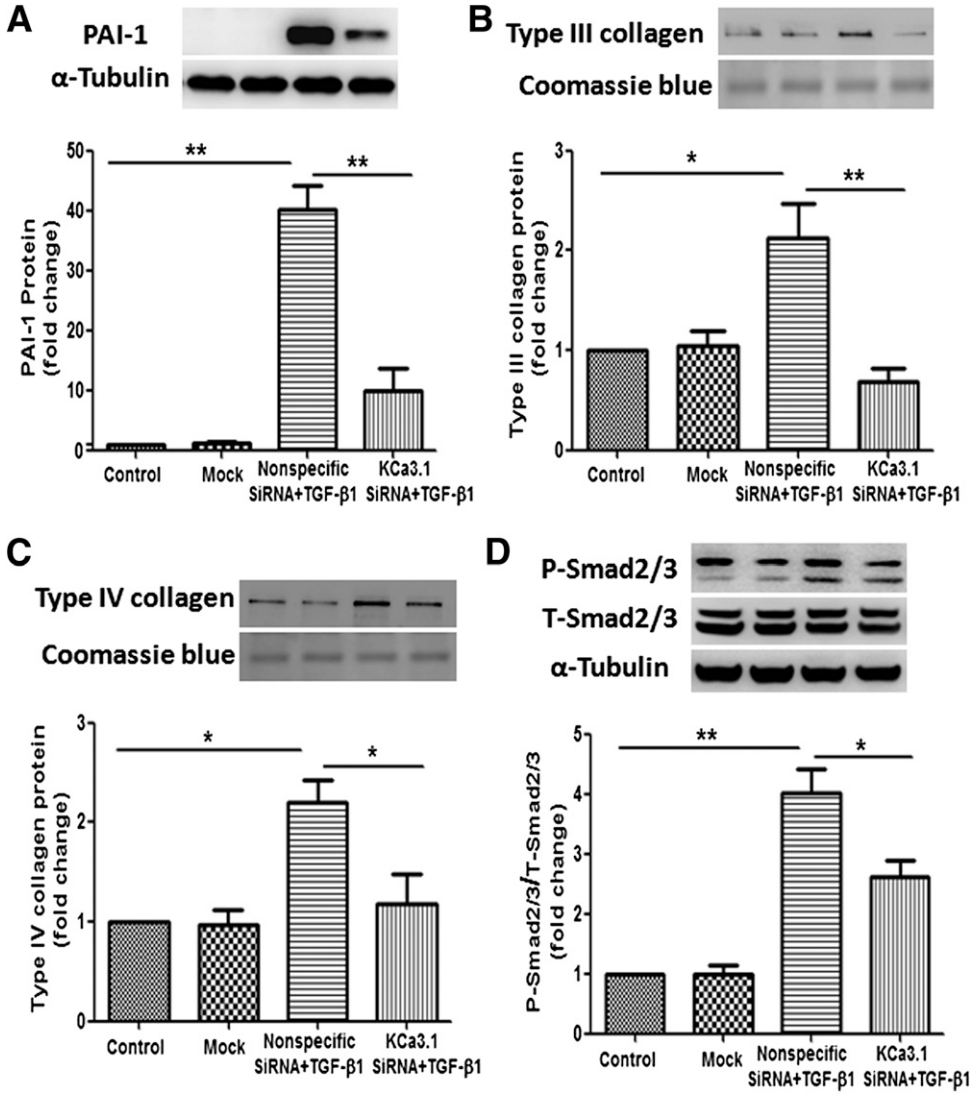

FIG. 5. Blockade of KCa3.1 inhibited TGF-β1–stimulated PAI-1 and type III and IV collagen expression via the Smad2/3 pathway in human proximal tubular cells. Western blots demonstrate that TGF-β1 increased the expression of PAI-1 (*A*) and type III (*B*) and IV collagen (*C*) and activated Smad2/3 phosphorylation (*D*) in cultured human proximal tubular cells (HK2 cells) at 48 h, which were reversed in KCa3.1 siRNA–transfected HK2 cells. TRAM34 suppressed TGF-β1–induced PAI-1 (*E*) and type III (*F*) and IV collagen (*G*) and phosphorylation of Smad2/3 (*H*) in HK2 cells. Results are presented as mean ± SEM. *$P < 0.05$; **$P < 0.01$. $n = 4$.

KCa3.1 deficiency significantly reduced their levels ($P < 0.05$) (Fig. 4*A–E*). Phosphorylation of Smad2/3 and its subsequent nuclear translocation are critical steps in TGF-β1 signaling; therefore, the TGF-β1–induced Smad2/3 signaling pathway was examined. As shown in Fig. 4*C*, immunohistochemical staining showed that TGF-β1–Smad2/3 signaling was strongly activated in diabetic KCa3.1$^{+/+}$ mice. However, the activation was inhibited in KCa3.1 deletion diabetic mice ($P < 0.01$) (Fig. 4*F*). Similarly, blockade of KCa3.1 with the administration of TRAM34 significantly decreased the expression of TGF-β1 and TβRII after diabetic injury ($P < 0.05$) (Fig. 4*G–K*) at both mRNA and protein levels. In addition, phosphorylation of Smad2/3 was suppressed in diabetic kidneys from TRAM34-treated mice compared with vehicle-treated mice ($P < 0.05$) (Fig. 4*I* and *L*). Taken together, these data indicate that KCa3.1 mediates expression of both TGF-β1 and its receptor, TβRII, through the Smad2/3 pathway in the diabetic kidneys.

Blockade of KCa3.1 inhibits TGF-β1–stimulated PAI-1 and type III and IV collagen expression via the Smad2/3 pathway in human proximal tubular cells. To support the in vivo findings reported above, human proximal tubular cells (HK2 cells) exposed to TGF-β1 were concurrently exposed to KCa3.1 siRNA or TRAM34, respectively. As expected, exposure of HK2 cells to TGF-β1 resulted in significantly increased expression of PAI-1 and type III and IV collagen compared with the control, whereas concurrent exposure to KCa3.1 siRNA or TRAM34 inhibited the TGF-β1–mediated increases in PAI-1 ($P < 0.05$) (Fig. 5*A* and *E*), type III collagen ($P < 0.01$) (Fig. 5*B* and *F*), and type IV collagen ($P < 0.05$) (Fig. 5*C* and *G*). In addition, phosphorylation of Smad2/3 in HK2 cells that had been exposed to TGF-β1 was inhibited by KCa3.1 siRNA or TRAM34 ($P < 0.05$) (Fig. 5*D* and *H*). These data suggest that the antifibrotic effect of KCa3.1 is mediated by the TGF-β1/Smad signaling pathway.

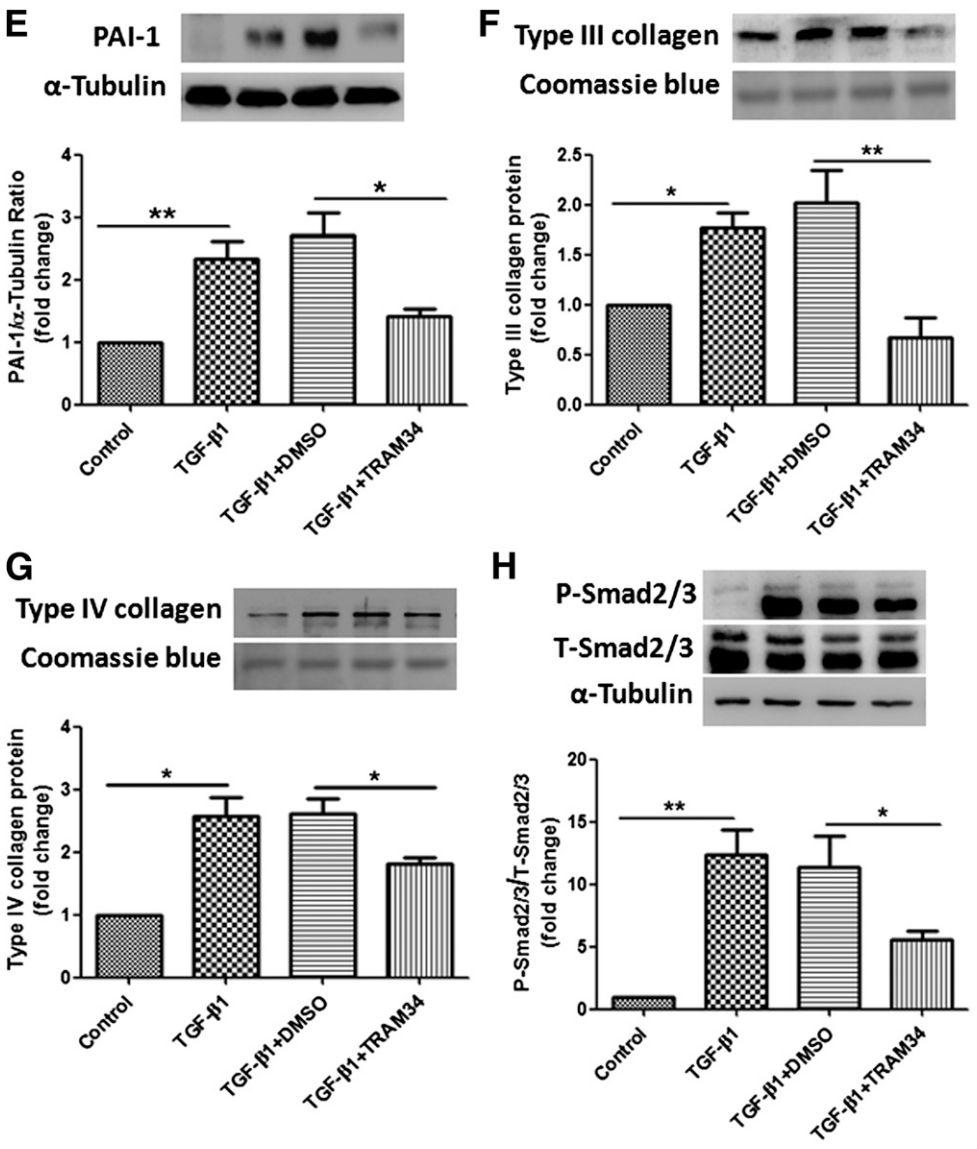

FIG. 5. Continued.

DISCUSSION

This study was undertaken to address whether inhibition of the calcium-activated potassium channel KCa3.1 will ameliorate renal dysfunction and attenuate the renal fibrosis inherent in diabetic nephropathy, and to elucidate the possible underlying mechanisms. Our studies have first demonstrated that KCa3.1 expression is increased in both human and mice models with diabetic nephropathy. Subsequently, our findings demonstrate that KCa3.1 deficiency significantly attenuated inflammation, regulators of matrix production, and matrix protein expression and thus reduces renal fibrosis in the KCa3.1 knockout mouse model of diabetic nephropathy. In addition, with administration of the KCa3.1 inhibitor TRAM34, a highly selective inhibitor of KCa3.1, we provided evidence that pharmacological inhibition of KCa3.1 was similarly effective in mitigating the development of renal fibrosis after diabetic injury, which implies an important role for KCa3.1 in the pathogenesis of renal fibrotic disease. Furthermore, in vitro results supported that blockade of KCa3.1 inhibited TGF-β1–induced fibrotic responses through Smad2/3-dependent pathways.

Calcium regulates a wide range of vital cell functions, including enzyme activities, attachment, motility, morphology, metabolic processes, cell-cycle progression, signal transduction, replication, gene expression, and electrochemical responses. It is well-known that pathophysiological inflammation is implicated in the progression of diabetic nephropathy. KCa3.1-mediated elevation of intracellular calcium is necessary for the production of inflammatory chemokines and cytokines by T cells, macrophages, and mast cells (29,30). Activation of KCa3.1 is believed to contribute to migration, activation, and proliferation of immunologically active cells. KCa3.1 expression is upregulated in activated naive and central memory T cells and IgD^+ B cells (31,32), and the channel has therefore been proposed as a target for the treatment of autoimmune diseases and transplant rejection (33). Recently, the combination of TRAM34 with the Kv1.3 blocking peptide ShK was further shown to reduce T-cell and macrophage infiltration in the early stages of

chronic kidney transplant rejection in rats (23), suggesting that KCa3.1 blockers may represent a novel alternative therapy for prevention of kidney allograft rejection. In this study, we observed that blockade of KCa3.1 inhibited infiltration of macrophage F4/80 and suppressed the expression of MCP-1 and ICAM1 in the diabetic kidneys. These results suggest that inhibition of inflammatory responses may be a key mechanism by which KCa3.1 attenuates renal fibrosis.

Inhibition of KCa3.1 may elicit an antifibrotic effect by multiple mechanisms. As TGF-β1 signaling has a central role in a variety of fibrogenic processes, such as ECM protein accumulation in diabetic nephropathy and tubulointerstitial fibrosis (31,34), we examined the effect of KCa3.1 on the expression of TGF-β1 and TβRII in the kidneys of mice with diabetic nephropathy. Our results clearly indicated that expression levels of TGF-β1 and TβRII mRNA were upregulated in the diabetic kidney, and inhibition of KCa3.1 suppressed their expression (Fig. 4). Thus, we suggest that KCa3.1-targeted inhibition of renal fibrosis is likely mediated by antagonizing TGF-β1 signaling through suppression of TGF-β1 and TβRII expression. To further elucidate the mechanism by which blockade of KCa3.1 inhibits inflammatory cytokine and matrix protein expression, we examined whether blockade of KCa3.1 inhibited TGF-β1–mediated Smad2/3 activity. TGF-β receptor, a transmembrane Ser/Thr kinase receptor, phosphorylates receptor-regulated Smads, such as Smad2/3. Phosphorylated Smads enter the nucleus, where they activate the expression of target genes, including PAI-1, and matrix proteins and subsequently contribute to tubulointerstitial fibrosis (35). In this study, we found that blockade of KCa3.1 successfully inhibited TGF-β1–stimulated target gene expression, including PAI-1; matrix proteins expression; and inflammatory cytokine expression through the Smad2/3 pathway. This study showed that the antifibrotic effects of KCa3.1 are at least partly mediated by the suppression of TGF-β1 signaling.

In summary, the current study is the first to report that blockade of KCa3.1 can inhibit excessive deposition of ECM and transcriptional expression of TGF-β1, TβRII, and several proinflammatory cytokines that are associated with diabetic nephropathy through Smad2/3 pathways. Therefore, inhibition of the KCa3.1 signaling pathway may provide a novel approach to prevent the development of diabetic nephropathy and attenuate the progression of renal fibrosis.

ACKNOWLEDGMENTS

This work was supported by an Australian National Health and Medical Research Council project grant (NHMRC APP1025918) and a University of Sydney Postgraduate Award (to C.H.).

No potential conflicts of interest relevant to this article were reported.

C.H. conceived and designed the research, performed and interpreted the results of experiments, analyzed data, prepared figures, and drafted and revised the manuscript. S.S., Q.M., J.C., and A.G. performed and interpreted partial experiments and revised the manuscript. C.A.P. and X.-M.C. conceived and designed the research, interpreted the results of experiments, and revised the manuscript. All authors approved the final version of the manuscript. C.A.P. is the guarantor of this work and, as such, had full access to all the data in the study and takes responsibility for the integrity of the data and the accuracy of the data analysis.

The KCa3.1$^{-/-}$ mice were kindly provided by Dr. James Melvin, National Institute of Dental and Craniofacial Research, Bethesda, MD.

REFERENCES

1. Rosolowsky ET, Skupien J, Smiles AM, et al. Risk for ESRD in type 1 diabetes remains high despite renoprotection. J Am Soc Nephrol 2011;22:545–553
2. Zheng H, Whitman SA, Wu W, et al. Therapeutic potential of Nrf2 activators in streptozotocin-induced diabetic nephropathy. Diabetes 2011;60:3055–3066
3. Wolf G. Growth factors and the development of diabetic nephropathy. Curr Diab Rep 2003;3:485–490
4. Prud'homme GJ. Pathobiology of transforming growth factor beta in cancer, fibrosis and immunologic disease, and therapeutic considerations. Lab Invest 2007;87:1077–1091
5. Ruster C, Wolf G. The role of chemokines and chemokine receptors in diabetic nephropathy. Front Biosci 2008;13:944–955
6. Stocker M. Ca(2+)-activated K+ channels: molecular determinants and function of the SK family. Nat Rev Neurosci 2004;5:758–770
7. Gardos G. The function of calcium in the potassium permeability of human erythrocytes. Biochim Biophys Acta 1958;30:653–654
8. Joiner WJ, Wang LY, Tang MD, Kaczmarek LK. hSK4, a member of a novel subfamily of calcium-activated potassium channels. Proc Natl Acad Sci USA 1997;94:11013–11018
9. Ishii TM, Silvia C, Hirschberg B, Bond CT, Adelman JP, Maylie J. A human intermediate conductance calcium-activated potassium channel. Proc Natl Acad Sci USA 1997;94:11651–11656
10. Logsdon NJ, Kang J, Togo JA, Christian EP, Aiyar J. A novel gene, hKCa4, encodes the calcium-activated potassium channel in human T lymphocytes. J Biol Chem 1997;272:32723–32726
11. Begenisich T, Nakamoto T, Ovitt CE, et al. Physiological roles of the intermediate conductance, Ca2+-activated potassium channel Kcnn4. J Biol Chem 2004;279:47681–47687
12. Chou CC, Lunn CA, Murgolo NJ. KCa3.1: target and marker for cancer, autoimmune disorder and vascular inflammation? Expert Rev Mol Diagn 2008;8:179–187
13. Hu L, Pennington M, Jiang Q, Whartenby KA, Calabresi PA. Characterization of the functional properties of the voltage-gated potassium channel Kv1.3 in human CD4+ T lymphocytes. J Immunol 2007;179:4563–4570
14. Tao R, Lau CP, Tse HF, Li GR. Regulation of cell proliferation by intermediate-conductance Ca2+-activated potassium and volume-sensitive chloride channels in mouse mesenchymal stem cells. Am J Physiol Cell Physiol 2008;295:C1409–C1416
15. Tharp DL, Bowles DK. The intermediate-conductance Ca2+ -activated K+ channel (KCa3.1) in vascular disease. Cardiovasc Hematol Agents Med Chem 2009;7:1–11
16. Toyama K, Wulff H, Chandy KG, et al. The intermediate-conductance calcium-activated potassium channel KCa3.1 contributes to atherogenesis in mice and humans. J Clin Invest 2008;118:3025–3037
17. Köhler R, Wulff H, Eichler I, et al. Blockade of the intermediate-conductance calcium-activated potassium channel as a new therapeutic strategy for restenosis. Circulation 2003;108:1119–1125
18. Wulff H, Kolski-Andreaco A, Sankaranarayanan A, Sabatier JM, Shakkottai V. Modulators of small- and intermediate-conductance calcium-activated potassium channels and their therapeutic indications. Curr Med Chem 2007;14:1437–1457
19. Ohya S, Kimura K, Niwa S, et al. Malignancy grade-dependent expression of K+-channel subtypes in human prostate cancer. J Pharmacol Sci 2009;109:148–151
20. Wulff H, Gutman GA, Cahalan MD, Chandy KG. Delineation of the clotrimazole/TRAM-34 binding site on the intermediate conductance calcium-activated potassium channel, IKCa1. J Biol Chem 2001;276:32040–32045
21. Wulff H, Miller MJ, Hansel W, Grissmer S, Cahalan MD, Chandy KG. Design of a potent and selective inhibitor of the intermediate-conductance Ca2+-activated K+ channel, IKCa1: a potential immunosuppressant. Proc Natl Acad Sci USA 2000;97:8151–8156
22. Grgic I, Kiss E, Kaistha BP, et al. Renal fibrosis is attenuated by targeted disruption of KCa3.1 potassium channels. Proc Natl Acad Sci USA 2009;106:14518–14523
23. Grgic I, Wulff H, Eichler I, Flothmann C, Köhler R, Hoyer J. Blockade of T-lymphocyte KCa3.1 and Kv1.3 channels as novel immunosuppression strategy to prevent kidney allograft rejection. Transplant Proc 2009;41:2601–2606
24. Tesch GH, Allen TJ. Rodent models of streptozotocin-induced diabetic nephropathy. Nephrology (Carlton) 2007;12:261–266

25. Livak KJ, Schmittgen TD. Analysis of relative gene expression data using real-time quantitative PCR and the 2(-Delta Delta C(T)) Method. Methods 2001;25:402–408
26. Doi S, Zou Y, Togao O, et al. Klotho inhibits transforming growth factor-beta1 (TGF-beta1) signaling and suppresses renal fibrosis and cancer metastasis in mice. J Biol Chem 2011;286:8655–8665
27. Brosius FC 3rd, Alpers CE, Bottinger EP, et al.; Animal Models of Diabetic Complications Consortium. Mouse models of diabetic nephropathy. J Am Soc Nephrol 2009;20:2503–2512
28. Liu Y. Renal fibrosis: new insights into the pathogenesis and therapeutics. Kidney Int 2006;69:213–217
29. Ghanshani S, Wulff H, Miller MJ, et al. Up-regulation of the IKCa1 potassium channel during T-cell activation. Molecular mechanism and functional consequences. J Biol Chem 2000;275:37137–37149
30. Cruse G, Duffy SM, Brightling CE, Bradding P. Functional KCa3.1 K+ channels are required for human lung mast cell migration. Thorax 2006;61:880–885
31. Li JH, Huang XR, Zhu HJ, Oldfield M, Cooper M, Truong LD, Johnson RJ, Lan HY. Advanced glycation end products activate Smad signaling via TGF-beta-dependent and independent mechanisms: implications for diabetic renal and vascular disease. FASEB J 2004;18:176–178
32. Wulff H, Calabresi PA, Allie R, et al. The voltage-gated Kv1.3 K(+) channel in effector memory T cells as new target for MS. J Clin Invest 2003;111:1703–1713
33. Chandy KG, Wulff H, Beeton C, Pennington M, Gutman GA, Cahalan MD. K+ channels as targets for specific immunomodulation. Trends Pharmacol Sci 2004;25:280–289
34. Isono M, Chen S, Hong SW, Iglesias-de la Cruz MC, Ziyadeh FN. Smad pathway is activated in the diabetic mouse kidney and Smad3 mediates TGF-beta-induced fibronectin in mesangial cells. Biochem Biophys Res Commun 2002;296:1356–1365
35. Huang Y, Noble NA. PAI-1 as a target in kidney disease. Curr Drug Targets 2007;8:1007–1015